

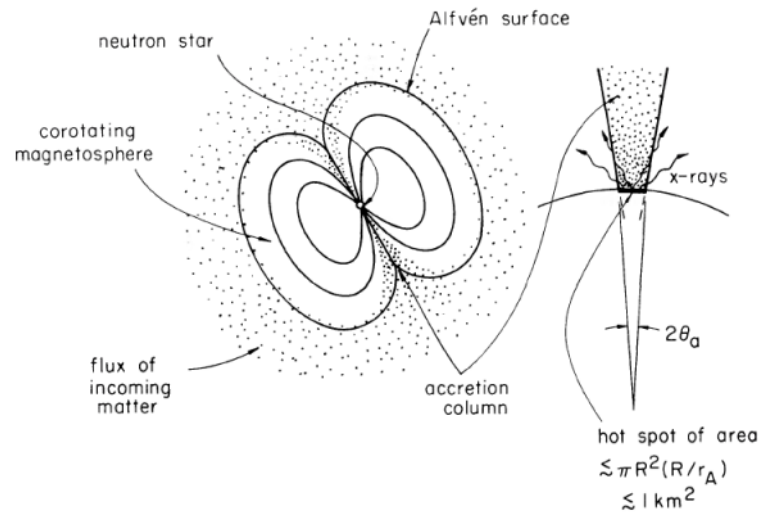
# X-ray Emissions from Magnetic Polar Regions of Neutron Stars

Hajime Inoue  
Meisei University

Since discoveries of Her X-1 (Giacconi et al. 1971) and Cen X-3 (Tananbaum et al. 1972) with Uhuru, more than 100 X-ray pulsars have been found.

## General consensus on situations of X-ray pulsars

- a close binary of a strongly magnetized neutron star + a normal star
- an accretion flow from the normal star to the neutron star
- a magneto-boundary surface at  $\sim 10^8$  cm where the magnetic pressure of the NS once stops the flow
- two channeled flows along magnetic funnels to the magnetic poles at the NS surface
- X-ray emissions from the polar regions at the NS surface
- an oblique rotation of the magnetic axis, causing X-ray pulsation



schematic diagrams by Lamb, Pethick & Pines (1973)

# Studies on structures of the polar X-ray emitting regions

Davidson (1973)

A simple treatment

kinetic energy  $\rightarrow$  radiation energy

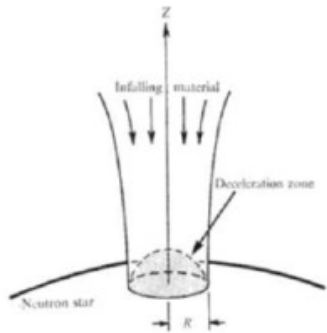


Fig. 1 Base of an accretion funnel. The  $z$  axis extends upward from a magnetic pole of the neutron star.

low accretion rate case



generalization to higher accretion rate



more detailed study to reproduce X-ray spectra

Becker & Wolff (2007)

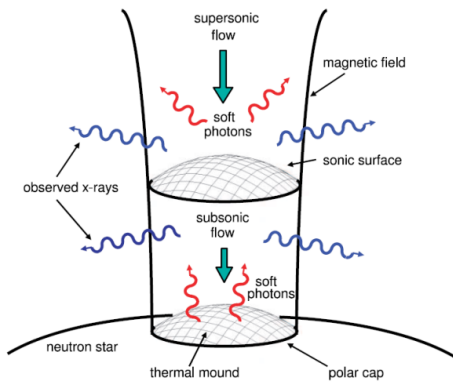


Fig. 1.—Schematic depiction of gas accreting onto the magnetic polar cap of a neutron star. Seed photons are created throughout the column via bremsstrahlung and cyclotron emission, and additional blackbody seed photons are emitted from the surface of the thermal mound near the base of the column.

Inoue (1975)

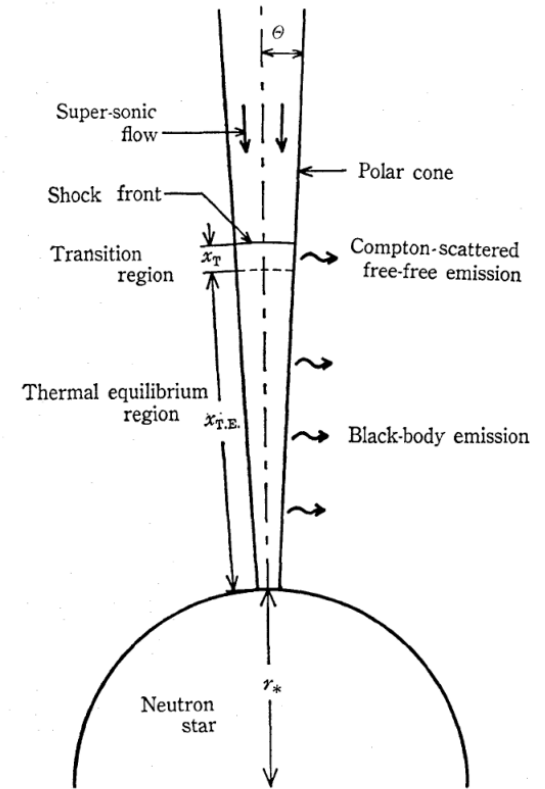


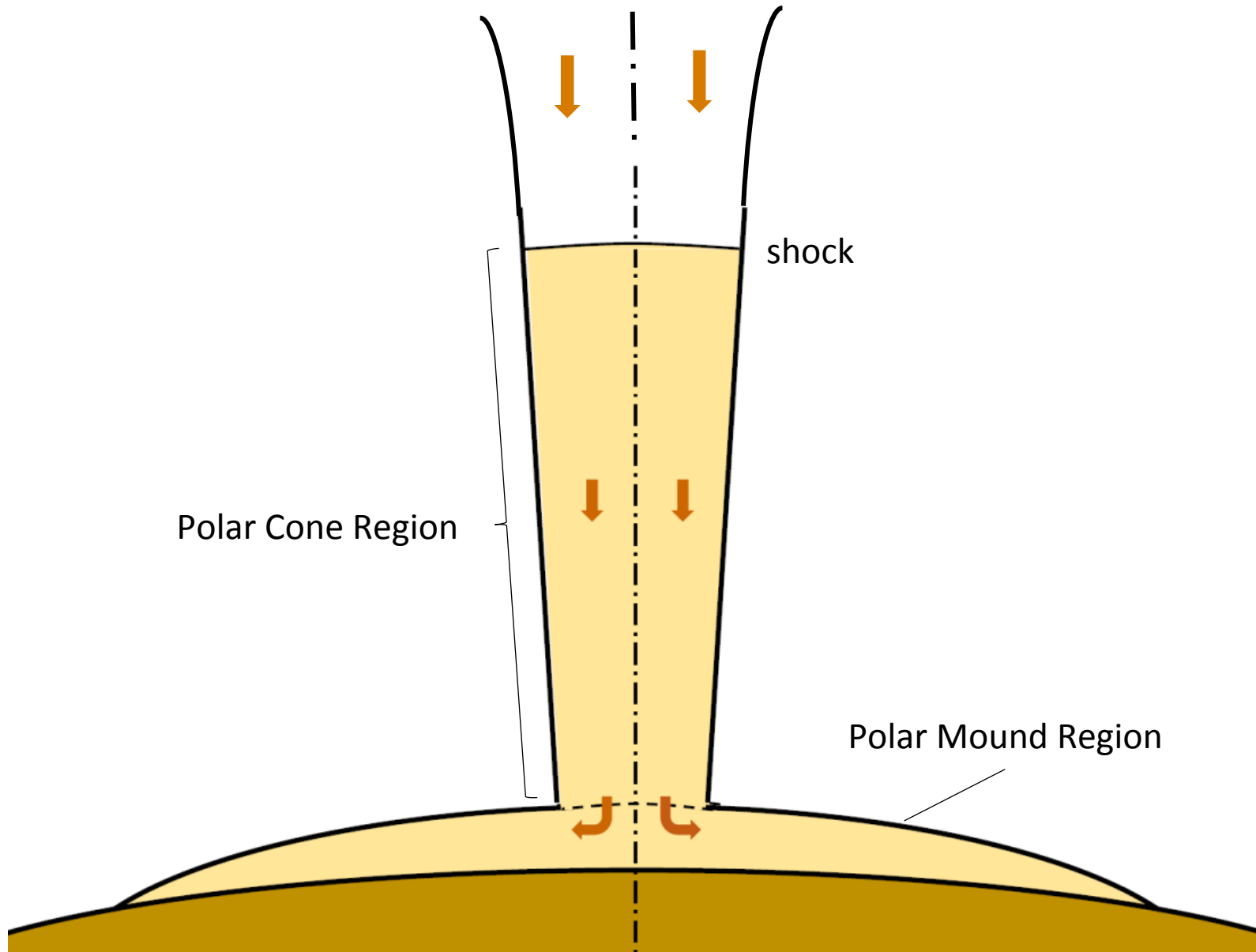
Fig. 1. Schematic diagram of the polar cone near the stellar surface.



more detailed study

This talk : Inoue (2019, in preparation)

# Model-configurations of an X-ray emitting polar region of a neutron star



# Model for accretion flow in the Polar Cone Region on a neutron star

## Assumptions

- quasi-radial, steady flow in a polar cone
- narrow cone  $\Theta \ll 1$   
averaged over a cross section of the cone
- radiation energy dominant  
 $P = U/3 = \frac{4}{3} \rho T^4 / 3$
- sufficiently subsonic  
kinetic energy  $\ll$  thermal energy
- energy loss : side-way diffusion of photons  
energy loss rate per volume :  $q$

$$q = U/t_D = \rho \epsilon \frac{4c}{3} T^4 (r\Theta)^2$$

## Equations

- mass flow continuity  $M/2 = \pi(r\Theta)^2 \rho v$
- pressure balance  $dP/dr = -\rho GM/r^2$
- energy Eq.  $M/2 \frac{d}{dr} \left( \frac{4}{3} \epsilon - \frac{GM}{r} \right) = \pi(r\Theta)^2 q = \frac{4}{3} \rho c T^4 \epsilon$

## Parameters

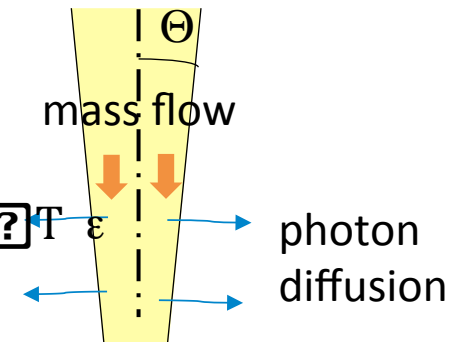
- $M/2$  accretion rate through the cone
- $M$  mass of the neutron star
- $r$  radial distance
- $\Theta$  opening angle of the cone
- $v$  inflow velocity
- $\rho$  matter density
- $P$  radiation pressure
- $U$  radiation energy density
- $\epsilon$  specific radiation energy density

$$\epsilon = U/3$$

- $t_D$  effective side-way diffusion time

$$t_D = \frac{4c}{3} \tau$$

$\tau = \kappa_T \rho(r\Theta)$  : optical depth  
 $\kappa_T$  : Thomson scattering opacity  
 $c$  : light velocity



Two differential equations on  $\epsilon$  and  $\rho$

pressure balance

$$dP/dr = -\rho GM/r^2 = U/3 = \frac{4\pi}{3} \rho r^2 \frac{d\epsilon}{dr} \quad \frac{d\epsilon}{dr} = -\frac{GM}{3r^3} \left( \frac{r}{r_D} + 3 \frac{GM}{r^2} \right)$$

energy Eq.

$$M/2 \frac{d}{dr} \left( \frac{4}{3} \epsilon - \frac{GM}{r} \right) = \pi (r \Theta)^2 q \approx \frac{4\pi}{3} r^2 \frac{d\epsilon}{dr} \left( \frac{r}{r_D} + 3 \frac{GM}{r^2} \right)$$

$$r_D = \frac{3 T}{8 c M} = 1.6 \times 10^5 \left( \frac{M}{M_{\odot}} \right)$$

Boundary conditions at the top of the Polar Cone

upper-stream side of the shock

free-fall approximation

$$v_1 = (2GM/r)^{1/2}$$

$$\rho_1 = M/2 \pi (r \Theta)^2 v_1 = M/2 \pi \Theta^2 (GM)^{1/2} r^{3/2} \quad \left( \frac{B^2}{8\pi} \right)_{\perp} \approx \frac{B_r^2}{8\pi} \quad B_{\theta}/B_r = \Theta$$

$$\epsilon_1 = v_1^2/2 = GM/r \quad (\text{specific matter energy})$$

**shock front (top side boundary)**

Radial distance of the top boundary:  $r_s$

Density at  $r_s$ :  $\rho_s$

$$\rho_s = 4 \rho_1(r_s)$$

Specific radiation energy density at  $r_s$ :  $\epsilon_s$

$$\frac{4}{3} \epsilon_s = \epsilon_1(r_s) = GM/r_s$$

Opening angle of the polar cone at  $r_s$ :  $\Theta_s$

(1) ram-pressure of the free-fall matter

$$\rho_1 v_1^2 = M/2 (2GM)^{1/2} / \pi \Theta^2 r^{3/2}$$

(2) magnetic pressure in the  $r$ -direction

$$\left( \frac{B^2}{8\pi} \right)_{\perp} \approx \frac{B_r^2}{8\pi} \quad B_{\theta}/B_r = \Theta$$

dipole approximation

$$B_r = B_{r,0} (r/R)^{-3}$$

$$B_{\theta} = B_r/2 \Theta \quad \Theta \ll 1$$

(1) = (2)

$$\Theta_s = \left( \frac{8(2GM)^{1/2} / (B_{r,0} R^3)^2}{\pi} \right)^{1/3} r^{7/6} \\ = 2.4 \times 10^{-3} \left( \frac{M}{10^{17}} \right)^{1/3} \left( \frac{M}{M_{\odot}} \right)^{1/6} \left( \frac{B_{r,0}}{10^{17} \text{ G}} \right)^{-2/3}$$

(cgs unit)

## Boundary conditions at the bottom of the Polar Cone

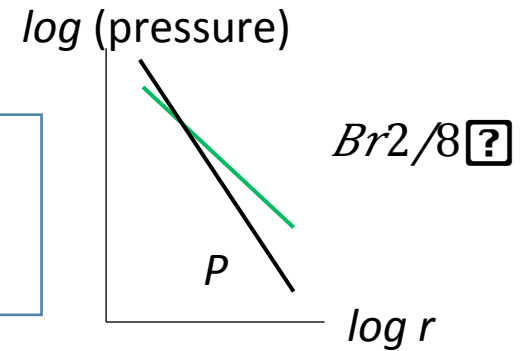
As shown next,

$$P \ll Br^2/8$$

$$|\log P / \log r| \gg |\log(8/Br^2) / \log r| \quad \text{on the top-side}$$



$P$  should exceed  $Br^2/8$ , somewhere.



## Boundary at the bottom of the Polar Cone

$r_B = R$  : the surface of the neutron star

$$P_B = \frac{B^2 R^3}{3} = Br,02/8$$

The conical configuration should end at the place where  $P_B = Br,02/8$ .

If  $P_B$  exceeds the magnetic pressure, the matter should push out the magnetic funnel.

We have searched a solution which satisfies the boundary condition,  $P_B = Br,02/8$ , at  $r=R$ , by changing the start position,  $r_s$ , in the numerical calculations.

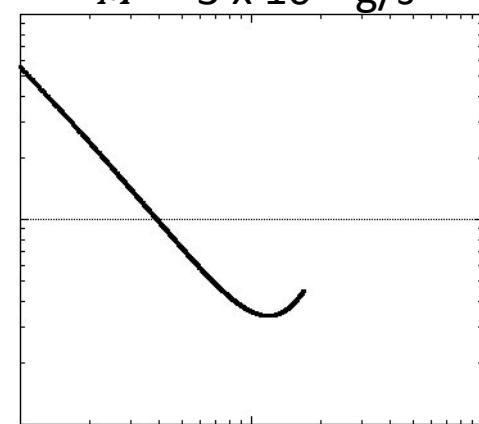
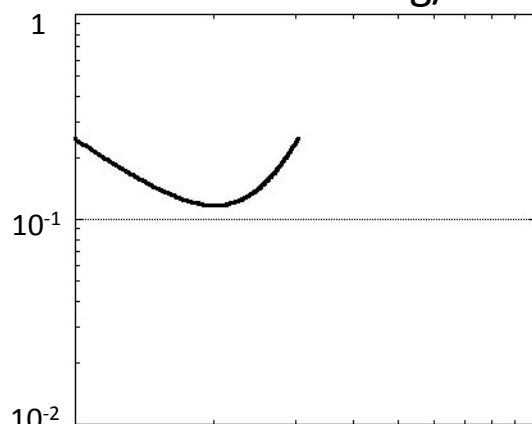
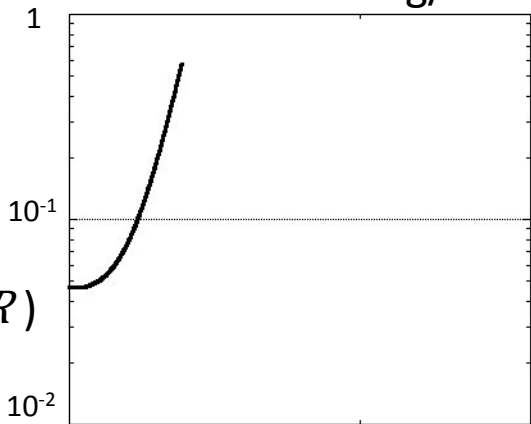
Solutions

$M = 3 \times 10^{16}$  g/s

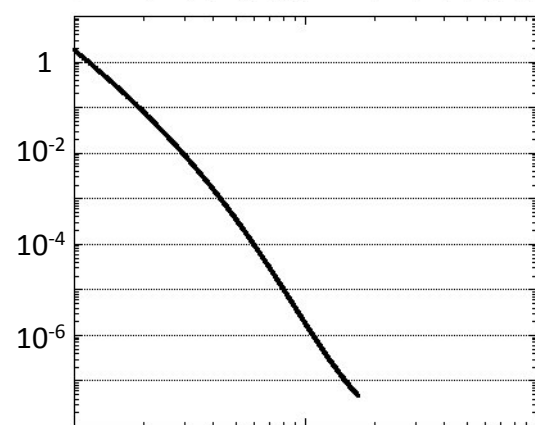
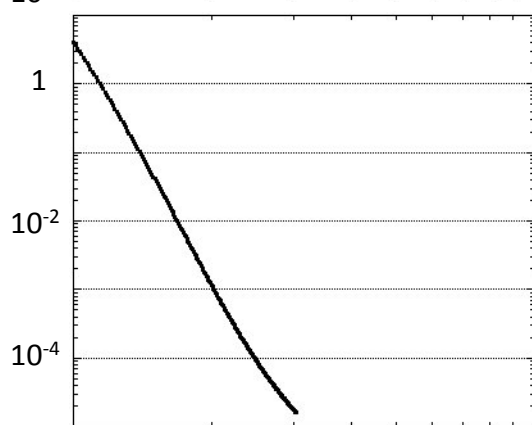
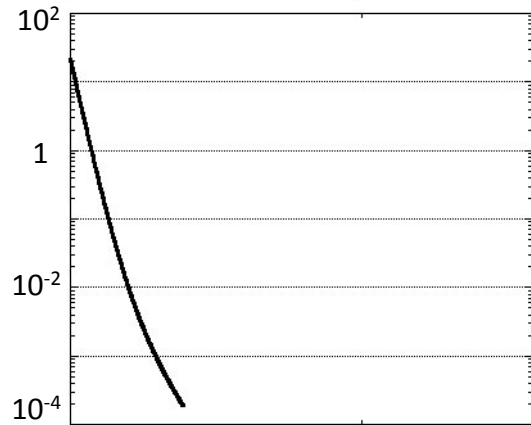
$M = 3 \times 10^{17}$  g/s

$M = 3 \times 10^{18}$  g/s

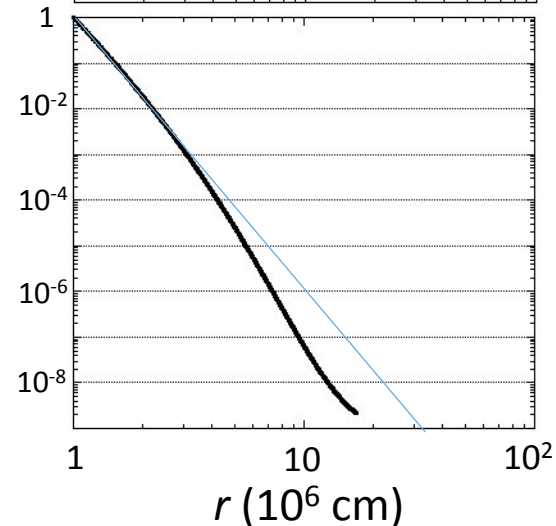
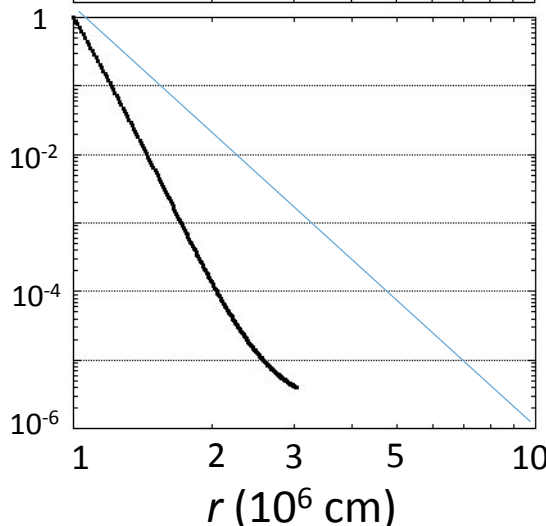
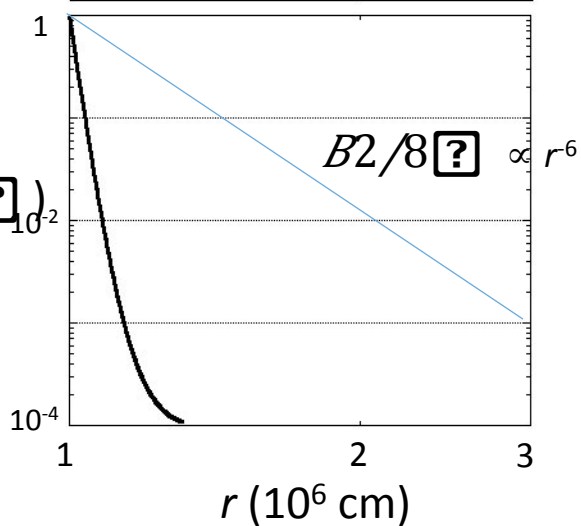
specific energy density  
( $\frac{E}{GM/R}$ )



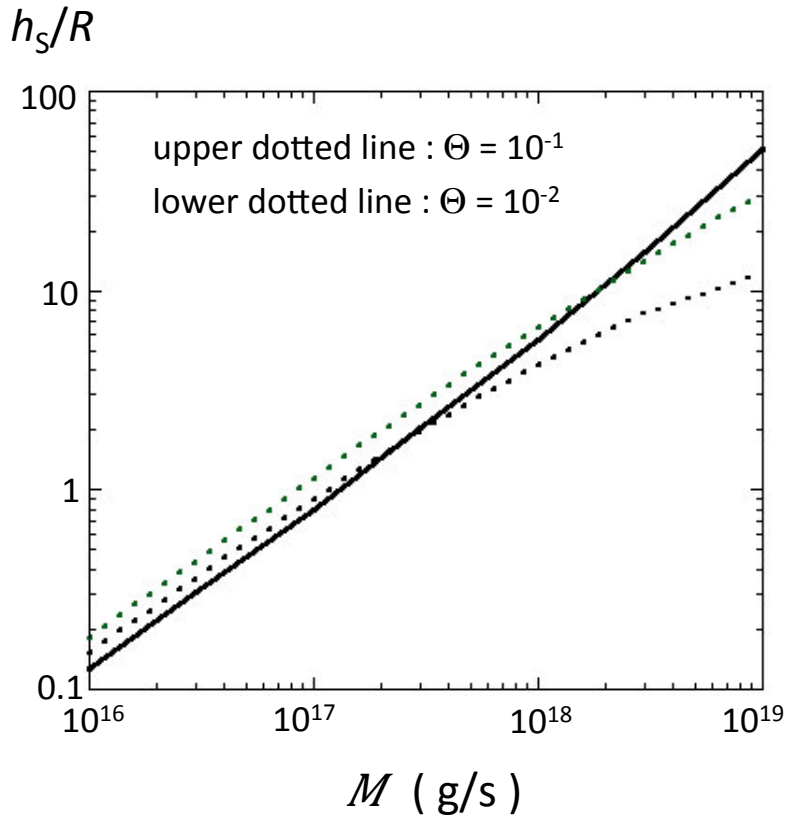
density  
(g/s)



pressure  
( $\frac{P}{B^2/8\pi}$ )



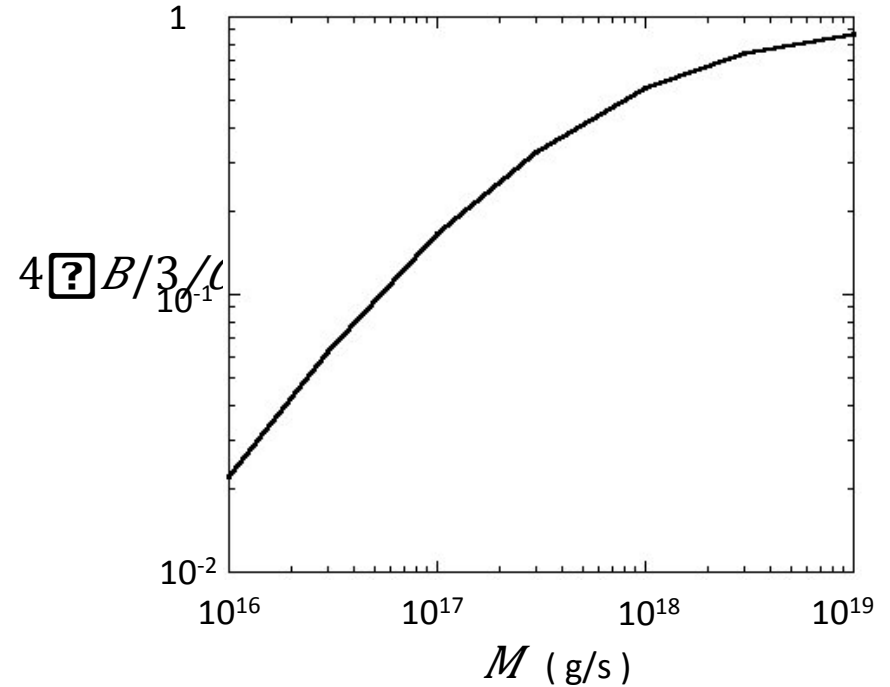
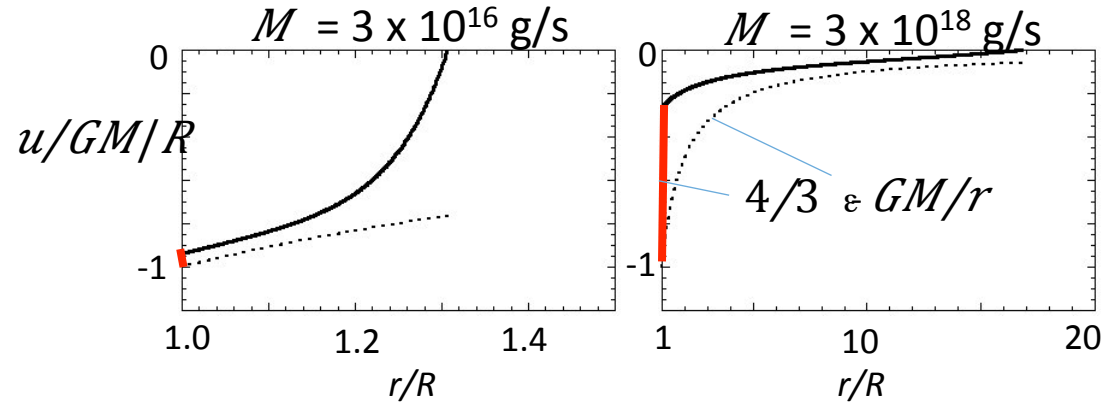
Height :  $h_s = r_s - R$   
 Opening angle :  $\Theta_s$  } of the Polar Cone



Two thin ( $\Theta \approx 0.1$ ) columns about 10 times as high as the neutron star radius stand when  $M \geq 10^{18}$  g/s.

Remaining thermal energy at the bottom of the PC

total specific energy :  $u = 4/3 \epsilon - GM/r$



Significant amount of thermal energy still remains at the bottom of the Polar Cone when  $M \approx 10^{18}$  g/s or more.

# Polar Mound region

The accreted matter still tends to go down with having significant amount of thermal energy at the bottom of the Polar Cone but its thermal pressure gets stronger than the magnetic pressure of the surrounding magnetic funnel below the bottom boundary.

Thus, the matter should start expanding radially along the surface of the neutron star with dragging the magnetic lines of force. We call this region as the Polar Mound region.

## Simple considerations on the structure of the Polar Mound

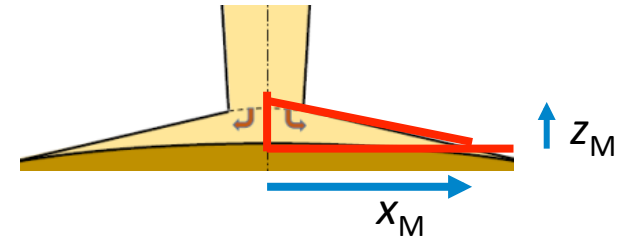
- The matter should radiate away the remaining thermal energy in this region to settle on the surface of the neutron star.

$$M/2 = M_{PM} = \frac{1}{3} \pi x_M^2 z_M \rho \text{ mass within the mound}$$

$$t_D = \frac{z_M}{c} \text{ photon diffusion time}$$

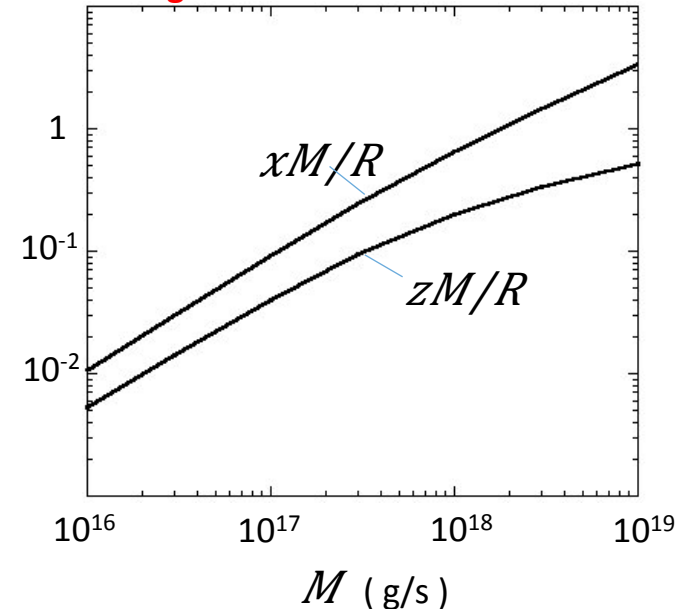
- The excess matter pressure should balance with the magnetic pressure strengthened by dragging.

$$P = P_0 \left( \frac{R - z_M}{R} \right)^{\xi} \quad B^2/8\pi = P_0 (x_M^2 + z_M^2)^{1/2} / z_M$$



Approximation : a cone with a radius,  $x_M$  and a height,  $z_M$

height and radius of the mound



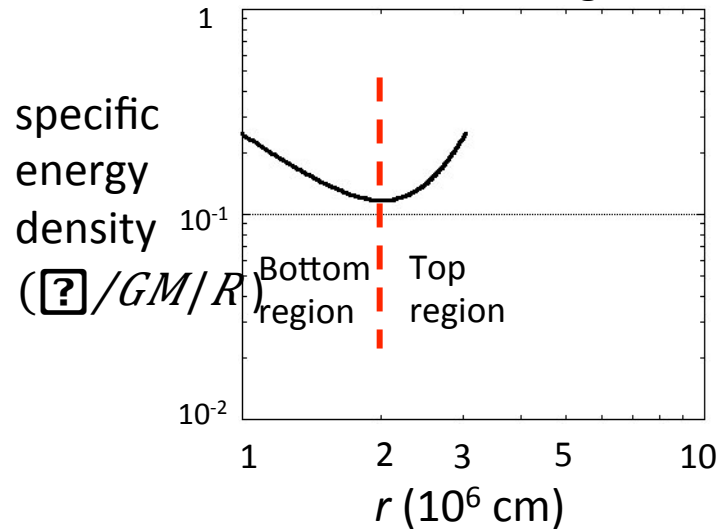
# Expected X-ray emission

## 3 components

I) 2 components from the Polar Cone

$$dL/dr = 4 \pi c / 3 T \epsilon$$

$$M = 3 \times 10^{17} \text{ g/s}$$

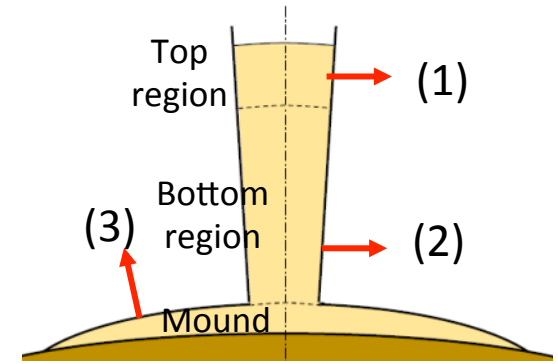


(1) X-rays from a region near the top boundary  
(behind the shock)

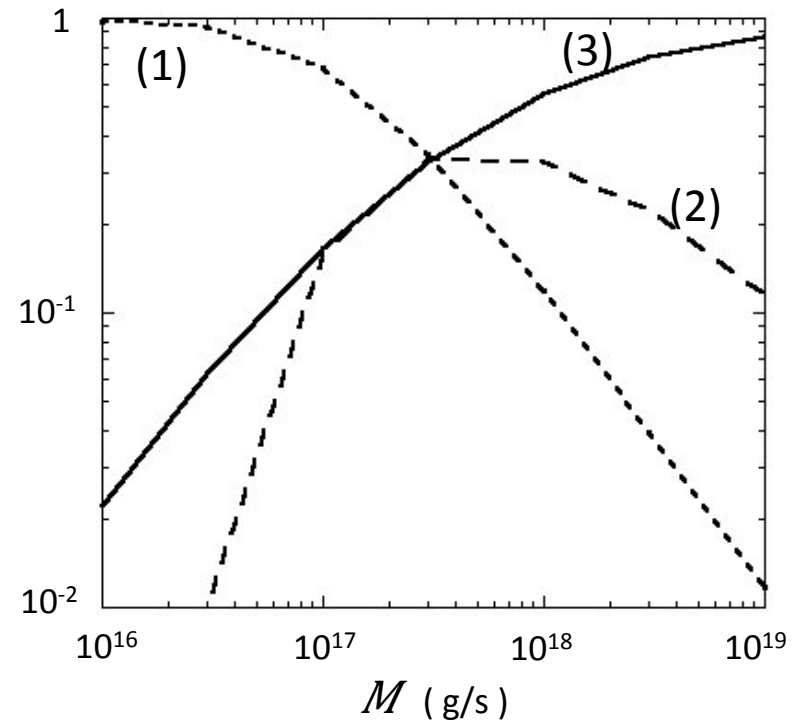
(2) X-rays from a region near the bottom boundary

II) 1 component from the Polar Mound

(3) X-rays from the Polar Mound

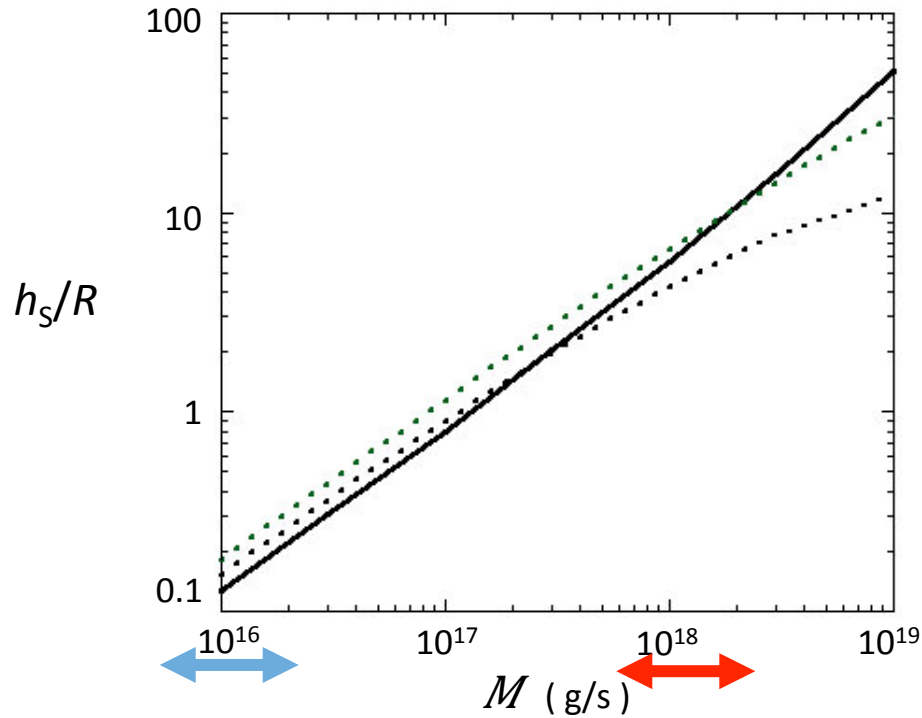


Proportions of the radiated energy of the 3 components

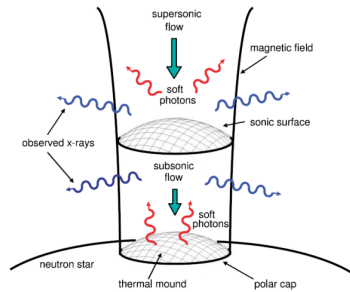


# Two typical cases of accretion rate

## Height of the Polar Cone



Case of low accretion rate :  $M \approx 10^{16}$  g/s

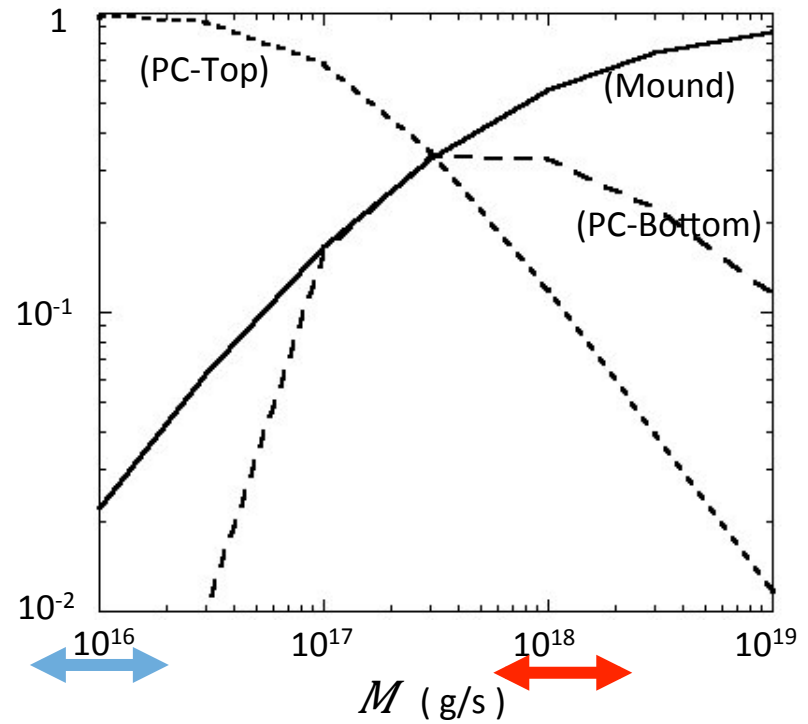


Emission from a region behind the shock

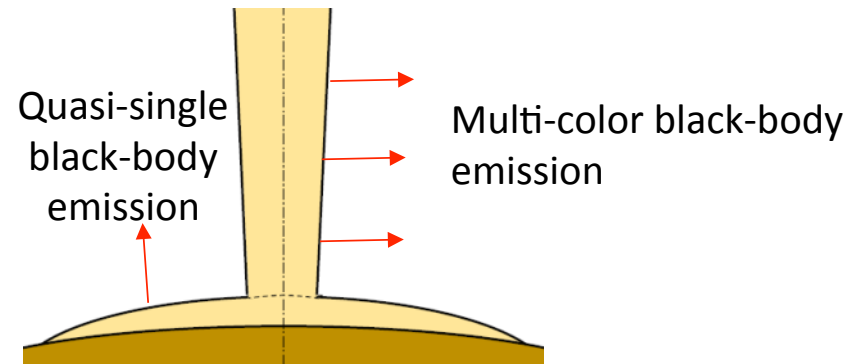
Becker & Wolff (2007)

FIG. 1.— Schematic depiction of gas accreting onto the magnetic polar cap of a neutron star. Seed photons are created throughout the column via bremsstrahlung and cyclotron emission, and additional blackbody seed photons are emitted from the surface of the thermal mound near the base of the column.

## Proportions of 3 emission components



Case of high accretion rate :  $M \approx 10^{18}$  g/s



# Expected X-ray spectrum

Bright X-ray pulsars

$$L \approx 10^{37} \sim 10^{38} \text{ erg/s}$$

$$M \approx 10^{17} \sim 10^{18} \text{ g/s}$$



2 component spectrum

a multi-color blackbody + a blackbody

"NPEX" model well reproduces observed spectra of several X-ray pulsars. (Makishima et al. 1999)

NPEX model

$$(A_n E^{-\alpha} + A_p E^2) \exp(-E/kT)$$

$E^{-\alpha} \exp(-E/kT) \sim$  multi-color blackbody spectrum

$$dLPC/dr = 4 \frac{c}{3} T \epsilon_\epsilon = \frac{2\pi^5}{15} \frac{\Theta^4}{c^3 r^\mu}$$



$$T_e \propto r^{-(\nu+\mu+1)/4}$$

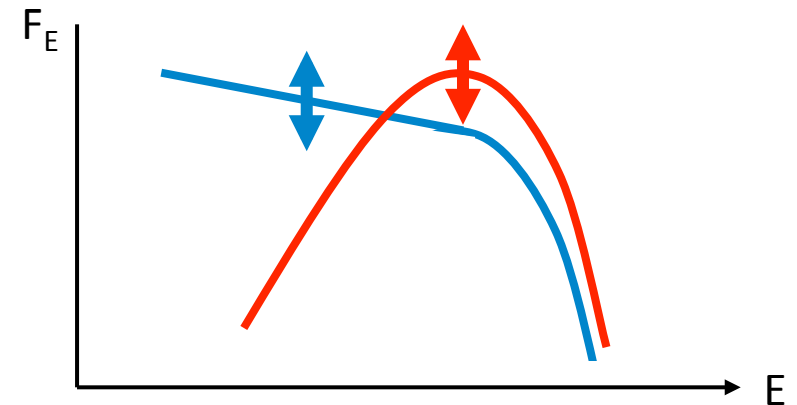
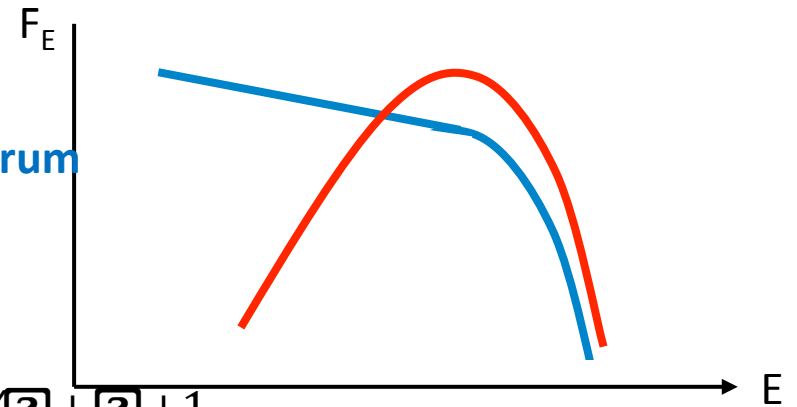


$$\alpha = 6 - 2(\nu + \mu) / (\nu + \mu + 1)$$

$E^2 \exp(-E/kT) \sim$  single blackbody spectrum

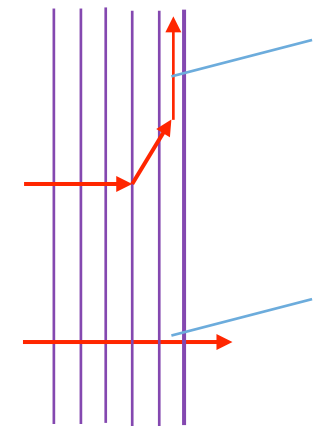
The 2-component spectrum of a multicolor blackbody + a blackbody well reproduces Her X-1 spectra in every pulse phases by changing only normalization factors.

(Kondo, Dotani & Inoue 2019, in preparation)



# Beam patterns of X-ray emissions

## X-ray beaming in the direction of the magnetic lines of force (Basko & Sunyaev 1975)



The diagram shows several vertical purple lines representing magnetic field lines. Two red arrows represent X-ray polarization directions. One arrow is horizontal, pointing to the right, and is labeled 'X-rays polarized perpendicular to the lines of force'. The other arrow is diagonal, pointing up and to the right, and is labeled 'X-rays polarized along the lines of force'. Two blue arrows point to the field lines with the text 'free from electron scattering'.

X-rays polarized along the lines of force

X-rays polarized perpendicular to the lines of force

free from electron scattering

free from electron scattering

X-rays originally polarized along the field lines tends to be beamed in the direction of the lines of force.

X-rays originally polarized perpendicular to the lines of force should be emitted without beaming.

central side of the Polar Cone

magnetic lines of force in the surface layer of the Polar Cone

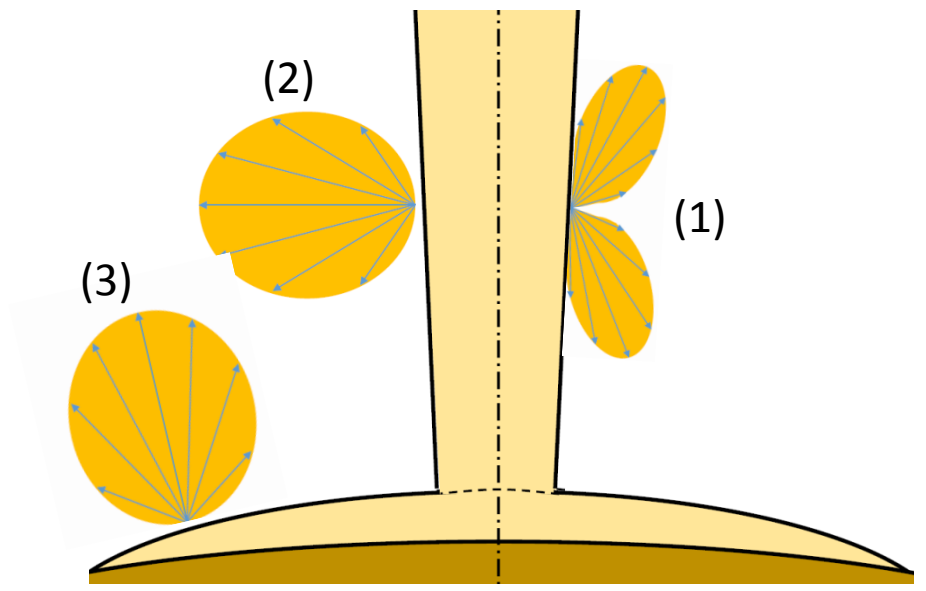
## 3 components in the beam pattern

I) 2 components from the Polar Cone region

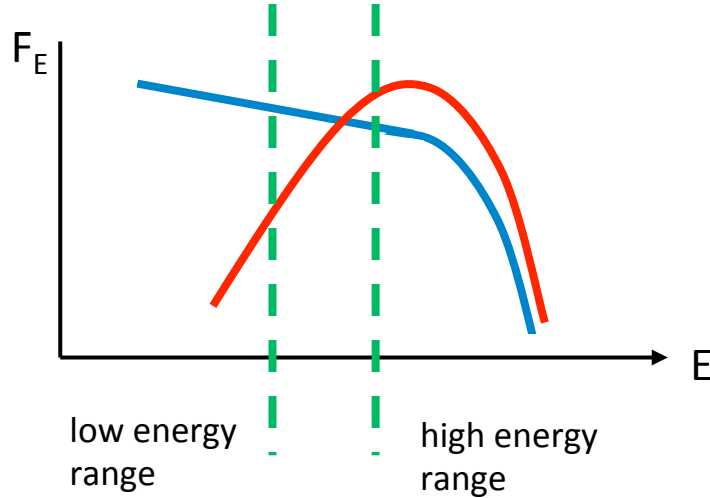
- 1) a narrow pencil beam
- 2) a broad fan beam

II) 1 component from the Polar Mound region

- 3) a broad pencil beam



## Expected pulse profiles



low energy range

Main: the narrow pencil beam  
from the Polar Cone

**possible to reproduce  
multiple peaks**

high energy range

Main: the broad pencil beam  
from the Polar Mound

Sub: the narrow pencil beam  
from the Polar Cone

## Observations

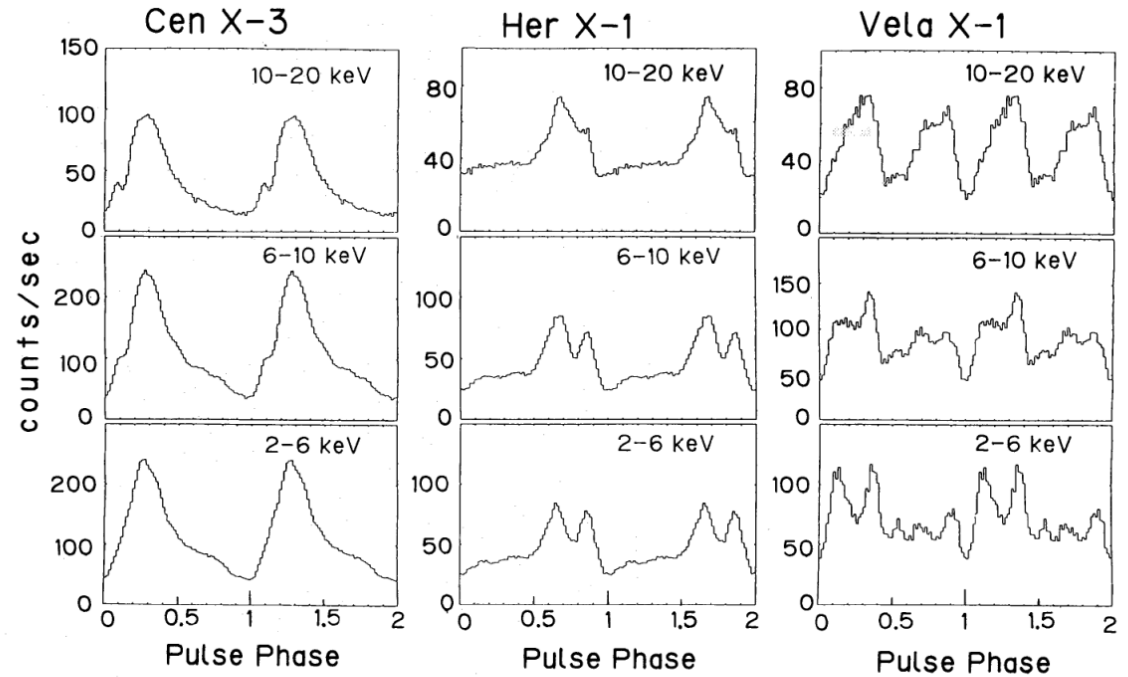
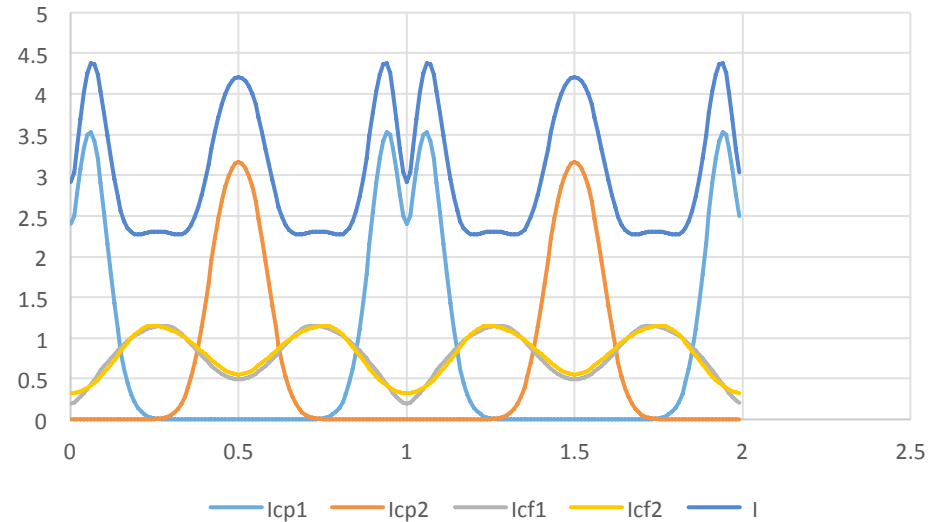
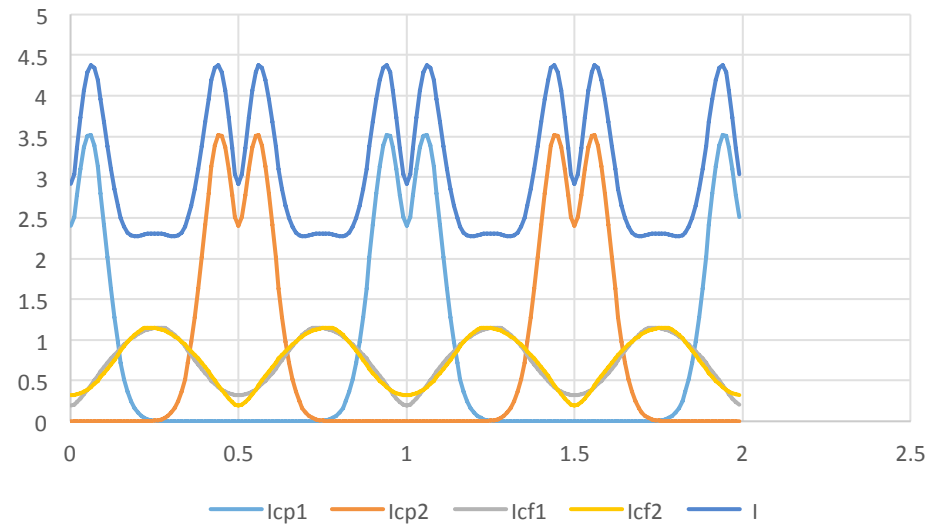
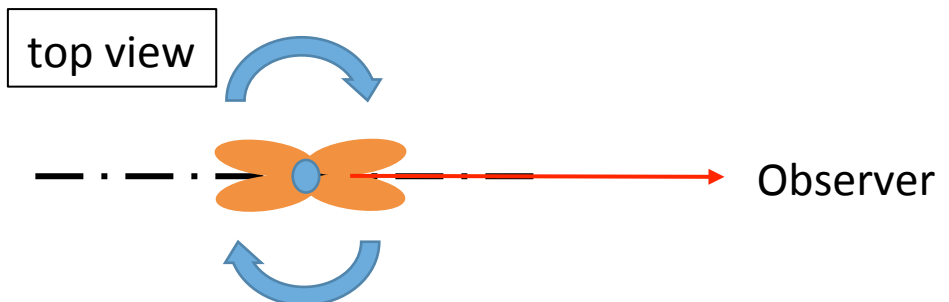
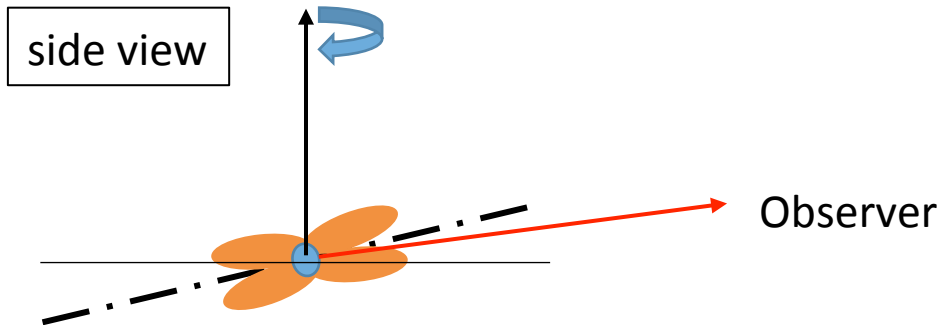
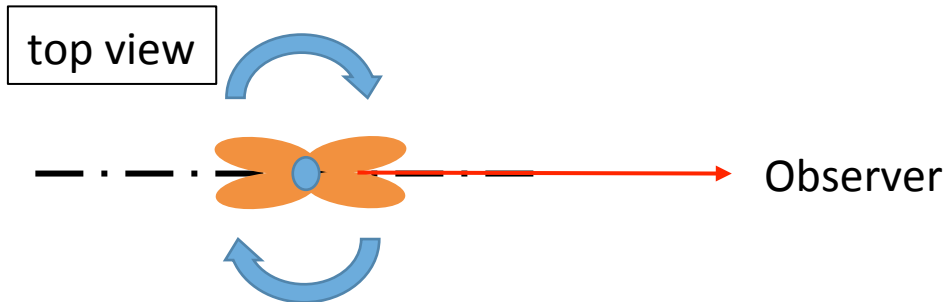
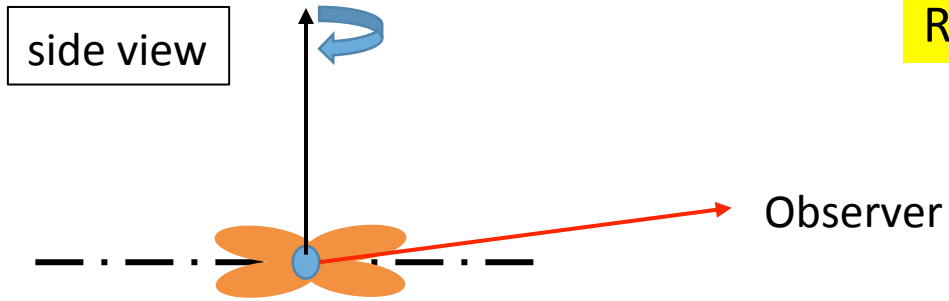


Fig. 3. Average pulse profiles observed by Tenma in three different energy bands for three typical X-ray pulsars, Cen X-3, Her X-1, and Vela X-1.

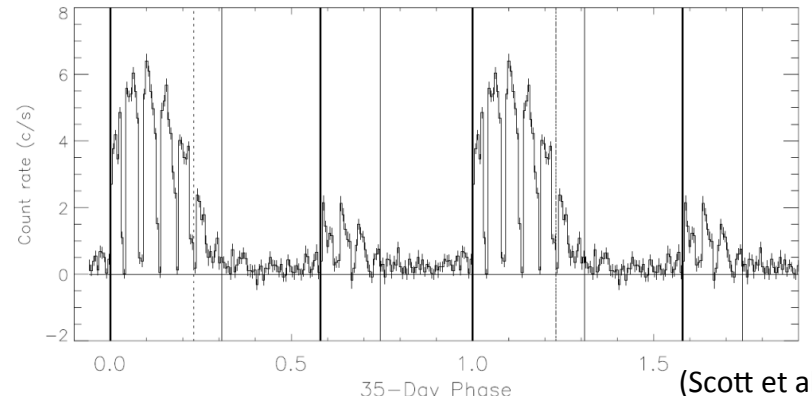
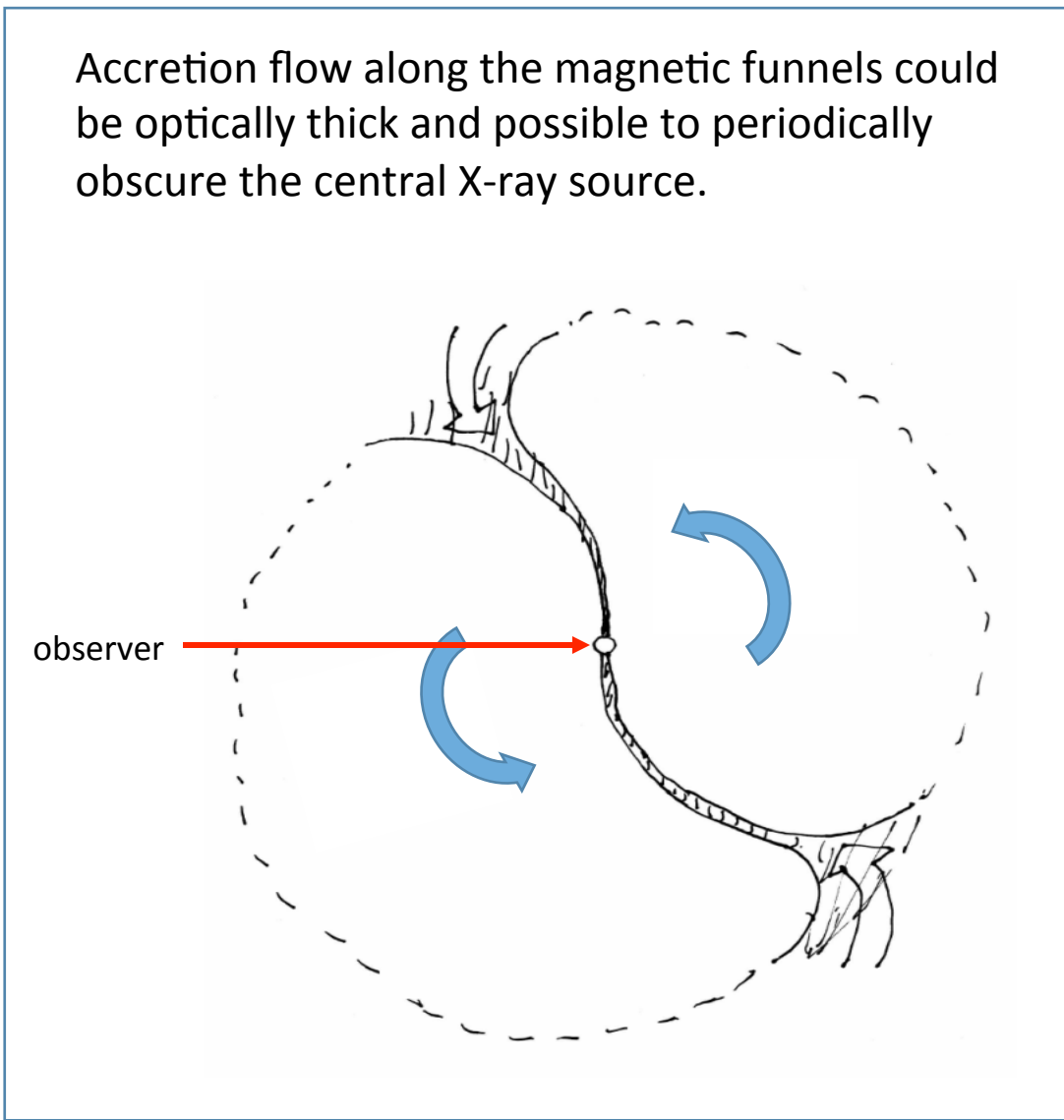
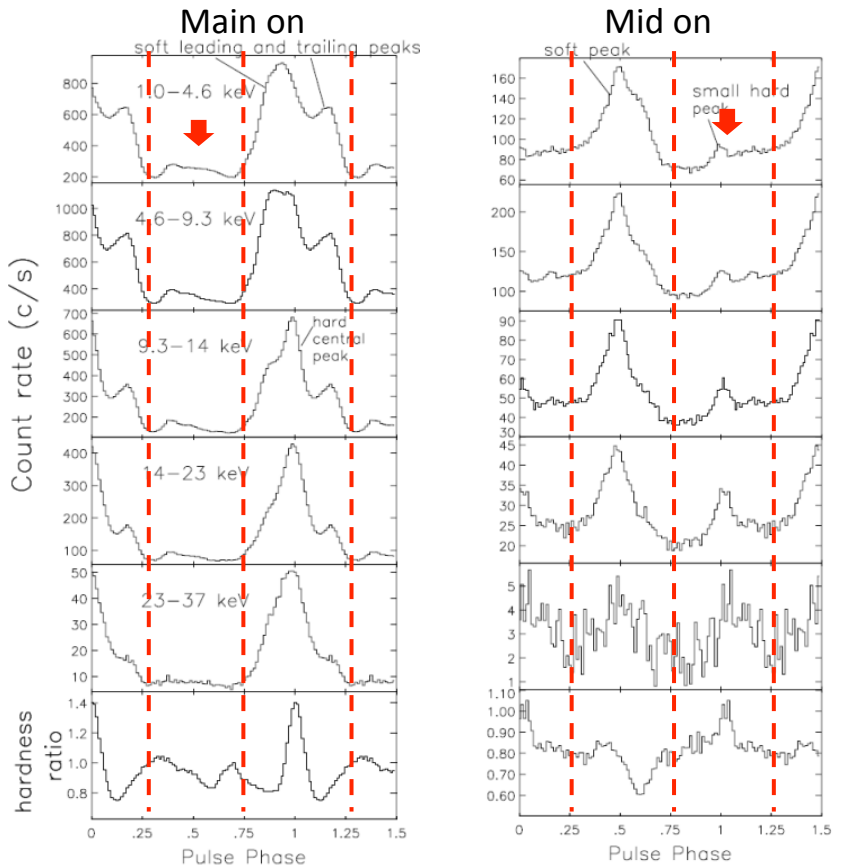
- (a) single sinusoidal-like shapes with little dependence on energy (X Per, GX 304-1 etc.),
- (b) sinusoidal-like double peaks with little energy dependence (GX 301-2, 4U 1538-52, SMC X-1 etc., the amplitudes of the two peaks are usually different),
- (c) an asymmetric single peak with some features (Cen X-3, GX 1+4 etc.),
- (d) a single sinusoidal-like peak at high and low energies and close adjacent double peaks in the intermediate energy range (Her X-1, 4U 1626-67 etc., the phase of maximum amplitude at low energies reverses by  $180^\circ$  with respect to that at higher energies for some sources), and
- (e) double sinusoidal-like peaks at high energies and complex five peaks at low energies (Vela X-1, A 0535+26 etc.).

# Results of a simple pulse profile calculation



Presence of phase-dependent obscuration → complications in reproduction of the pulse profiles

Pulse profile variation of Her X-1 associated with the 35-day cycle



(Scott et al. 2000)

## Summary

I have studied structures and properties of an X-ray emitting magnetic polar region on a neutron star composing of a polar cone region and a polar mound region

This model can qualitatively explain basic characteristics of observed X-ray spectra and pulse profiles of bright X-ray pulsars.

